Front. Struct. Civ. Eng. 2022, 16(9): 1071–1088
https://doi.org/10.1007/s11709-022-0879-0

RESEARCH ARTICLE

Thermal response of steel framing members in open car park fires

Xia YAN[a], Marion CHARLIER[b], Thomas GERNAY[a*]

[a] *Department of Civil and Systems Engineering, Johns Hopkins University, Baltimore, MD 21218, USA*
[b] *ArcelorMittal Steligence, Esch-sur-Alzette 4221, Luxembourg*
[*] *Corresponding author. E-mail: tgernay@jhu.edu*

ABSTRACT For open car park structures, adopting a performance-based structural fire design is often justified and allowed because the fire does not reach flashover. However, this design approach requires an accurate assessment of temperatures in structural members exposed to car fires. This paper describes a numerical study on the thermal exposure on steel framing members in open car park fires. Steel temperatures are computed by the coupling of computational fluid dynamics and finite element modeling, and by analytical models from the Eurocodes. In addition, the influence of galvanization on the steel temperature evolution is assessed. Results show that temperatures in unprotected beams and columns are influenced by the section geometry, car fire scenario, modeling approach, and use of galvanization. Galvanization slightly delays and reduces peak temperature. Regarding the different models, CFD-FEM (CFD: computational fluid dynamics, FEM: finite-element method) coupled models predict lower temperatures than the Hasemi model, because the latter conservatively assumes that the fire flame continuously touches the ceiling. Further, the Hasemi model cannot account for the effect of reduced emissivity from galvanization on the absorbed heat flux. Detailed temperature distributions obtained in the steel members can be used to complete efficient structural fire designs based on the member sections, structure layout, and use of galvanization.

KEYWORDS open car park, localized fire, steel frame, numerical modeling, computational fluid dynamics

1 Introduction

Car park buildings, which can be aboveground or underground, stand-alone or attached to other occupancy buildings, fully open or partially open, are commonly found in building environments. Open car parks, as defined based on ventilation conditions, are one of the most common types of car park buildings. Assessing the fire safety of open car parks requires an accurate representation of the fire events.

Car park fires have been studied in several recent experimental campaigns [1–3]. Heat release rates and temperatures were measured with different types and numbers of vehicles, as well as different car park layouts [2,4,5]. Heat release rate curves were proposed from full-scale experiments with different types of vehicles. Reference documents such as the Guidebook from CTICM [1] define reference fire scenarios with up to seven cars involved, for the design of open car parks subjected to fires. As flashover is unlikely to happen, a spatially uniform temperature field (e.g., from a zone model) does not capture the thermal exposure conditions for the structure. Instead, localized fire models are required to simulate burning cars and assess the heating of adjacent structural members.

In structural fire design, modeling of localized fires is either based on simple models, e.g., the models by Heskestad [6], Hasemi [7], and LOCAFI [8], which each have their field of application; or on advanced numerical modeling such as computational fluid dynamics (CFD) [9]. Simple and advanced models have been applied to capture thermal exposure from vehicle fires on bridges [10,11] and tunnels [12–14]. Recently, Yan and Gernay [15] conducted a benchmark study of simple models and coupled CFD-FEM methods against three localized fire experiments, from which a decision flowchart was

Article history: Received Apr 14, 2022; Accepted Jun 16, 2022

proposed to guide selection of the applicable model for capturing the thermal exposure from localized fires on structures.

Several recent studies have been carried out on the fire development in open structures. Khan et al. [16] studied the differences between conventional localized fires and the localized burning in large compartments and introduced the concept of semi-confined fire considering the compartment effects into localized fire models. Hidalgo et al. [17] characterized the transition of fire modes in a full-scale fire test carried out in an open-plan industrial building. Three distinct fire modes were identified including a traveling fire, a growing fire, and a fully developed fire, by the ratio between the flame front velocity and burnout front velocity. Nadjai et al. [18] conducted large scale fire tests to investigate the development of a traveling fire in open structures in the frame of the European RFCS-TRAFIR project and concluded that the positioning of the traveling fire band and the ceiling height directly influenced the temperatures reached in the surrounding structures. Alam et al. [19] conducted a second traveling fire test of the European RFCS-TRAFIR project with different open ventilation conditions. They found out that reduced opening size retained more heat within the compartment and induced higher temperatures in the surrounding steel structures. These studies highlight the importance of understanding the behavior of realistic fires in open structures and their impact on the surrounding structures.

However, limited research investigated the fire response of car park structures. The Hasemi model was used to analyze the thermal effect from burning vehicles on a steel beam at the ceiling level [20], and to conduct a thermal-mechanical analysis of the robustness of multi-story car parks under vehicle fires [21]. Sommavilla and Tondini [22] used both the Hasemi model and LOCAFI model to study the fire performance of a steel open car park subjected to the fire scenario relevant for the columns. Advanced analysis with the Fire Dynamic Simulator (FDS) was also used to investigate the fire spread and smoke movement in a large underground car park [23] and to conduct a coupled FDS-FEM analysis of an underground car park structure subjected to different fire scenarios with six burning cars [24]. A study by Tondini et al. showed that application of the Hasemi model led to more conservative thermal actions than the FDS-FEM coupling [25]. While these studies provided insights into the thermal response of structural members in car park fires, with the exception of the latter, they did not compare the temperatures predicted by different modeling approaches. Further, the effect of steel galvanization on the temperature rise in steel framing members has not been studied in the context of open car park fires. In theory galvanization is expected to affect the heat transfer through a reduction of the emissivity. There is interest in quantifying these effects and comparing simple and advanced modeling approaches as an accurate evaluation of the temperature development in the steel members. It is a crucial step in a performance-based structural fire design.

This study focuses on the analysis of the temperatures reached in open car park steel framing members under fire scenarios. The parameters considered in the analysis include the dimensions of the steel members, layout of burning vehicles, galvanization of the steel members, and the modeling approaches adopted. Both the simple analytical localized fire models and the advanced CFD-FEM coupling methods are used to evaluate the member temperatures. The predicted member temperatures by different modeling approaches are compared and discussed. Temperatures obtained can be used in structural FE analyses to design open car park structures for the fire situation. This study explores the benefits and limitations of simple models and exhibits the potential benefits of advanced numerical analysis for the performance-based design of open car parks in fire conditions.

2 Scope of the study

2.1 Car park layout and structure

Performance-based design approaches are well suited for a behavior assessment of open car parks in case of fire. Localized fire models are applied to represent the burning cars and assess the heating of the adjacent structural members. Indeed, in open car parks, a flashover is unlikely to happen and considering uniformly distributed temperatures is thus not deemed to properly represent the fire event. This observation, however, does not hold for underground car parks, or above-ground car parks with few openings (i.e., not meeting the requirements to be classified as open). The definition of an open car park depends on the country or jurisdiction under consideration [26], but it usually relies on a ratio of openings to surface of the boundaries of enclosure. Openings present on opposite façades also have an influence.

To conduct the parametric study on the temperatures reached in typical steel framing members under open car park fires, a medium-sized multi-story open car park is adopted [25]. The distance between the floor and the bottom part of the ceiling is 2.5 m. The floor plan of the car park is 60 m × 48 m, with 5 m × 2.5 m standard parking bays. The structure is a steel-concrete composite structure with steel framing and concrete flat slabs. One situation is based upon a steel hot rolled profile IPE450 for the beam (common design in composite steel-concrete car parks for 16 m primary beams spaced 2.5 m apart). Another one considers a steel hot rolled profile HE600A (common design for 16 m primary beams spaced 5 m

apart) [25]. The column is an HE240M hot rolled steel profile [22] and the concrete slab has a thickness of 0.2 m. The dimensions of the IPE450, HE600A, and HE240M profiles are shown in Fig. 1. No fire protection is applied to the structure.

To study the influence of galvanization on steel temperatures, the analysis is conducted for both ungalvanized profiles (UNGALVA) and galvanized profiles (GALVA). The emissivity of ungalvanized steel is taken as 0.7, independent of temperature, according to EN 1993-1-2 [27]. The thermal behavior of the galvanized steel is the same as that of ungalvanized steel except that the emissivity is 0.35 up to first heating to 500 °C, and 0.7 beyond. This is because the zinc coating applied on the surface of the steel irreversibly melts at a temperature of 500 °C.

2.2 Fire scenarios

The heat release rate (HRR) for burning cars is adopted from the CTICM recommendation as the HRR curve for a Class 3 car [1]. The classification of cars is based on the potential calorific value of cars [28]. According to the study by INERIS [29], Class 3 cars can be used to evaluate the structural stability of open car parks under fire, with the requirement that the stability of the structure should be ensured during the whole fire scenario. The heat release rate of a Class 3 car was experimentally obtained from a car fire test campaign conducted in 1995 at the CTICM laboratory. The Class 3 car equipped with four tires, one spare tire, and 2/3 tank of fuel were tested under a calorimetric hood in their operating state and showed a maximum heat release rate of 8.3 MW during the test. The car was ignited with 1.5 L of petrol in an open tray under the left front seat. The fire started at the front and remained stable for about the first 15 min. Then it spread to the rear part and reached the peak about 25 min after the ignition. The heat release rate was calculated with oxygen consumption techniques. Variation in testing car and testing method may lead to different heat release rate measurements, but the reference curves by CTICM have been widely used in car fire simulation, thus adopted in this study [20–22,30].

For the heating of the steel beams, three scenarios are considered that involve between one and three burning cars, as shown in Fig. 2. In the first scenario, a single car is burning, and it is positioned right below the beam. In the second scenario, a single car is burning, but with an offset from the axis of the beam. This layout is representative of situations where the beam is located above the boundary between two adjacent car park bays. In the third scenario, three cars are burning underneath the beam, and the axis is aligned with the middle car. When multiple cars are involved in a fire scenario, a time shift of fire propagation between nearby cars is observed [28]. Thus, the ignition of cars next to the first car igniting the fire is delayed by 12 min. In the third scenario in this study, the car in the middle is the first to ignite, followed by the two other cars after a delay of 12 min [28].

The Guidebook from CTICM [1] also recommends a scenario with seven cars placed transversally when studying the fire response of open car park beams. An analysis is conducted to verify whether higher temperatures are reached in the beam section when burning cars are located transversally in the axis of the beam, compared with the scenario 3 (Fig. 2) which has burning cars located transversally to the beam axis. Preliminary thermal analyses were conducted in OZone [31] with three cars and five cars arranged transversally. Indeed, localized fire models, in accordance with Annex C in

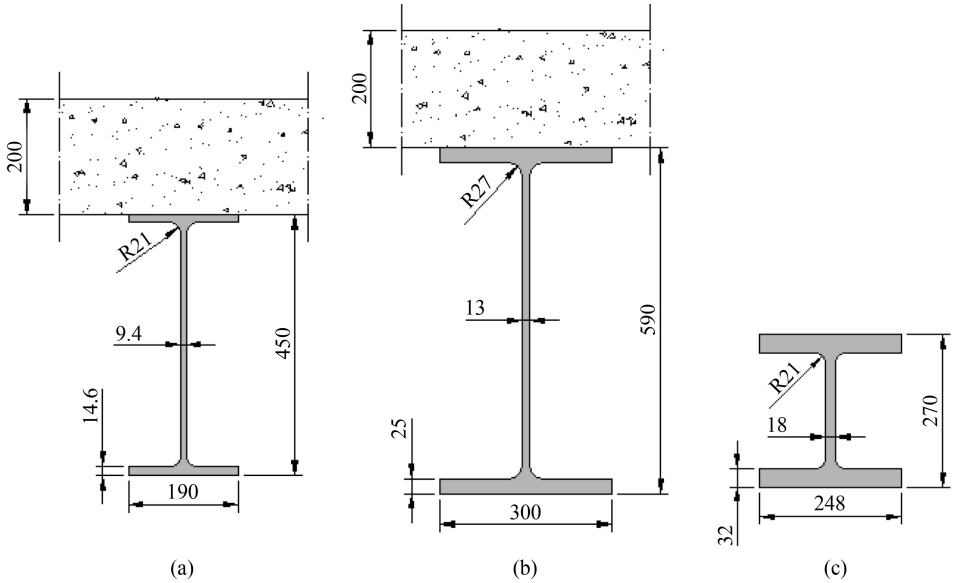

Fig. 1 Dimensions of the steel profiles (unit: mm). (a) IPE450; (b) HE600A; (c) HE240M.

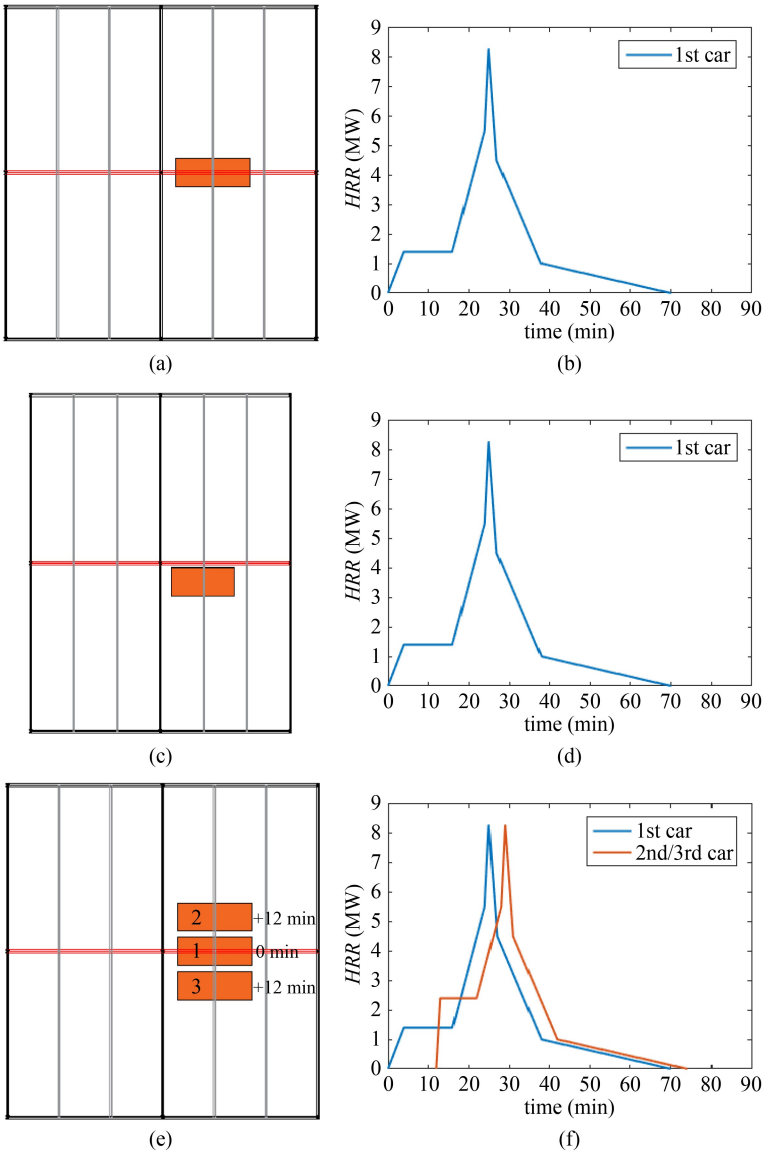

Fig. 2 Fire scenarios considered for the modeling of the thermal exposure on steel beams (burning cars are shown in orange, structure of interest is shown in red). (a) Plan view of scenario 1; (b) heat release rate; (c) plan view of scenario 2; (d) heat release rate; (e) plan view of scenario 3; (f) heat release rate.

EN1991-1-2 [32] were applied in OZone to analyze the temperature in the mid-span cross-section of both the ungalvanized IPE450 and HE600A profiles. The OZone analysis shows that peak temperatures reached locally with five burning cars are the same as those with three burning cars, as shown in Fig. 3, indicating that the burning cars far away from the structural member have marginal impact. Since the present study considers the heat modeling at a given section, the scenario with seven cars was not further considered.

For the steel columns, the considered scenario has the column located in the middle of 4 car park spots [1]. The four cars parked around the column become involved in the fire as shown in Fig. 4. The fire starts from one car, and spreads to the adjacent cars with a delay of 12 min. Finally, the car on the diagonal from the first ignited car starts burning at the 24th minute from the start. The heat release rate of each burning car follows the CTICM curve.

3 Methods for fire-thermal modeling

3.1 Selection of the modeling approach

Both simple models and advanced modeling approaches are available for analyzing car fire exposure on open car park structures. Detailed discussions and benchmarking against test data for the fire-thermal modeling approaches are provided in a recent study by the authors [15]. A summary of the models is provided hereafter.

The simple models in this study include the Heskestad,

Hasemi, and LOCAFI models. The Heskestad model is used to evaluate the flame temperature along the vertical centerline of the fire when the flame is not impacting the ceiling (e.g., for columns coinciding with the centerline of the fire or for part of the beam located just above the fire). The Hasemi model evaluates the heat flux received by the unit surface area at the ceiling level when the flame touches the ceiling (e.g., for beams or for column tops). The LOCAFI model calculates the radiative heat flux received by a vertical member not engulfed in the fire area (e.g., a column). As these models have different scopes of application, the selection of the applicable simple model results from the situation which is under consideration.

Advanced numerical modeling approaches rely on CFD to simulate the localized fire. A commonly used tool is FDS [9]. There are two main approaches to interface an FDS simulation with a subsequent FEM thermal analysis. The first uses the concept of Adiabatic Surface Temperature (AST) to summarize and transfer the thermal boundary information [33]. It assumes the surface to be a perfect insulator and the net heat flux is thus zero.

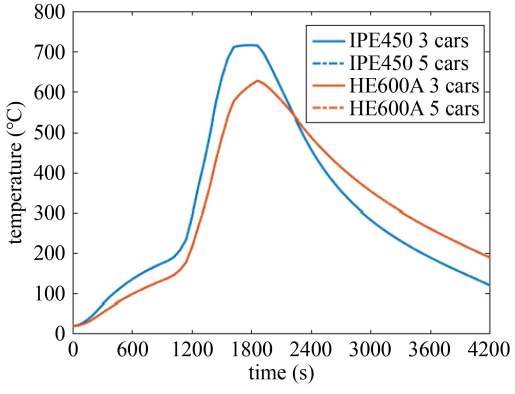

Fig. 3 Temperature in IPE450 and HE600A beams when subjected to 3 and 5 burning cars positioned transversally to the beam axis, as calculated with OZone (localized fires). The temperature curves for 3 and 5 cars for a given profile are superposed.

The fictitious temperature T_{AST} is calculated based on the incident radiative heat flux and the gas temperature near the surface [34]. Then the T_{AST} is applied to the FEM thermal analysis as thermal constraints. This method is referred to as the FDS-FEM AST method. The second method is referred to as the FDS-FEM interface method. It uses a transfer file containing the gas temperature and radiant intensities in the field of interest in FDS in a format readable by the FEM software [25]. Then the transfer file is read by the FEM software that interprets the quantities in terms of heat boundary conditions [35].

Figure 5 shows the applicable fire models based on the configuration between the localized fire and the steel member. The steel beams at the ceiling are inside the smoke layer [15]. When using simple models for analyzing beam sections outside the fire area (section 'B1' and 'B2'), the heat flux should be taken from the Hasemi model. However, if beam sections are inside the fire area (section 'B3'), the heat flux should be taken as the maximum between the Hasemi flux and the flux computed based on the flame temperature from the Hesketad model.

For steel beams, when selecting CFD-based modeling approaches, the FDS-FEM AST method is applicable to all configurations. The structural frame members should be included in the FDS model when adopting the AST method. The FDS-FEM interface method is applicable for structural members that are far from the fire source (section 'B1'); the relevant distance being such that the presence of the structural members does not noticeably affect the continuity of the temperature and radiative fields. These frame members should be omitted in the FDS model when using the interface method [15]. The ability to omit the frame members from the FDS simulation and to rely on an automatic transfer file between FDS and a FEM software is advantageous in terms of modeling effort. For sections closer to the heat source, which significantly influence the mass flow or radiative flow in the compartment (section 'B2'), the frame members should be included in the FDS model.

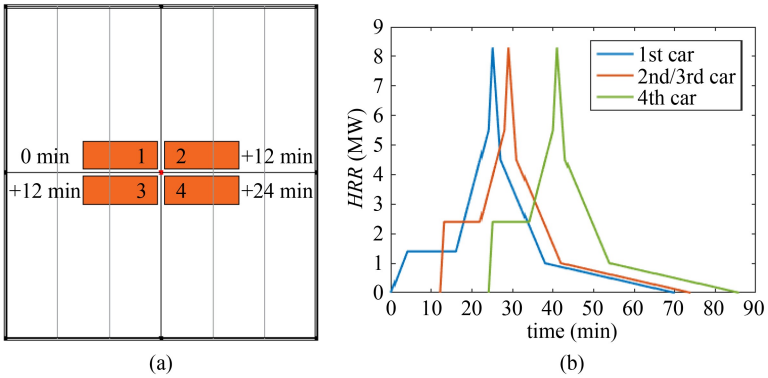

Fig. 4 Fire scenarios considered for the modeling of the thermal exposure on the steel column (burning cars are shown in orange and structure of interest is shown in red). (a) Plan view; (b) heat release rate.

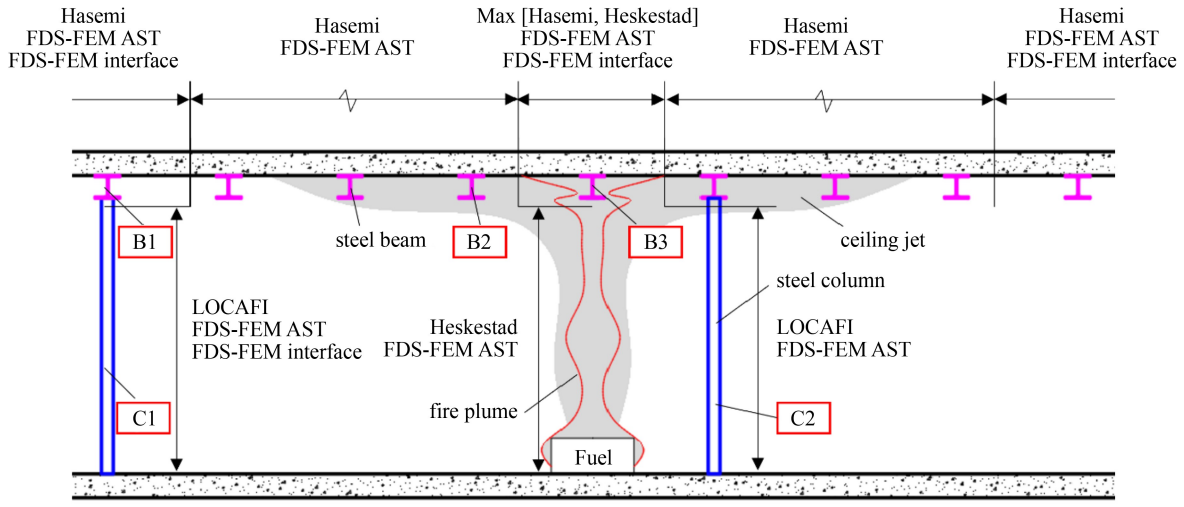

Fig. 5 Application domain of localized fire modeling approaches for car park fires (not to scale).

The AST method is preferred for the transfer of thermal information; except if the section is right above the heat source (section 'B3'), in which case owing to symmetry both FDS-FEM AST and FDS-FEM interface methods are applicable.

The steel columns of a car park are outside the fire area (burning car), and a distinction is made based on the position of the column in the smoke layer. For the lower part, which is outside the smoke layer, the surrounding gas is at ambient temperature or close to ambient temperature. Hence the convective part of the received heat flux can be neglected, and since the radiative heat flux is dominant, the LOCAFI model is applicable [22]. For the upper part of a column, which is inside the smoke layer, the convective heat flux from the hot smoke is not negligible, so the Hasemi model should be applied. When selecting CFD-based models, the FDS-FEM AST method is applicable regardless of the respective configuration between the column and the fire, but requires including the column in the FDS model and using a sufficient amount of AST sensors around the sections. When the column is away from the fire and the presence of the column does not impact the fire development (column 'C1'), the FDS-FEM interface provides an alternative method; the column is omitted from the FDS model in that case.

3.2 Fire analysis

The computational domain in FDS is 30 m × 22.5 m × 3 m (length × width × height) for the simulations of fire scenarios for the steel beam, as shown in Fig. 6. It is 20 m × 10 m × 3 m (length × width × height) for the simulations pertaining to the steel column. A sensitivity analysis is conducted on the computation domain to minimize the border effects with respect to the smoke flow. Burning cars are modeled as rectangular blocks with dimension of 4.8 m × 1.8 m × 0.3 m each. The heat release rate of the burning car is taken as the heat flux curves in Figs. 2 and 4. Based on research for car fires, the soot yield is set to 0.22 [36], and heat of combustion is set to 44.4 MJ/kg, typical of gasoline [25]. A mesh size of 0.1 m × 0.2 m × 0.1 m is selected. The special resolution $R^* = \mathrm{d}x/D^*$, where $\mathrm{d}x$ is the characteristic length of a cell for a given grid and D^* is the characteristic diameter of a plume, calculated with the selected mesh size falls into a reasonable range of 1/10–1/20 [9].

The heat transfer analysis to the steel member is conducted in the FEM software SAFIR [37]. The software SAFIR allows applying thermal boundary conditions to the surfaces of the steel members which are imported from FDS simulations or from the simple localized fire models provided in the Eurocodes, i.e., Hasemi, Heskestad, and LOCAFI (i.e., solid flame) [38].

To transfer thermal boundary information from FDS to the FEM software, two methods are used: the adiabatic surface temperature (AST) and the automatic interface. The steel member is included in the FDS analysis when using the AST method, while it is not included when using the interface method. To capture the thermal gradient, 14 sensors are attached onto the structural surface of cross sections at an interval of 0.2 m in the longitudinal direction to measure the AST. Then, the AST outputs from FDS are applied onto the 2D thermal model as thermal constraint for the FEM thermal analysis. For the interface method, the gas temperature and radiant intensities are output from FDS at the grids surrounding the structural member with a time step of 10 seconds and written into a transfer file. A sensitivity analysis is conducted on the time step at which the information from FDS is transferred to the FEM thermal analysis, confirming that 10 s is an adequate tradeoff for this problem. The transfer file is applied onto the 2D thermal model in SAFIR as thermal constraint. Then, 2D thermal analyses are conducted at each longitudinal integration

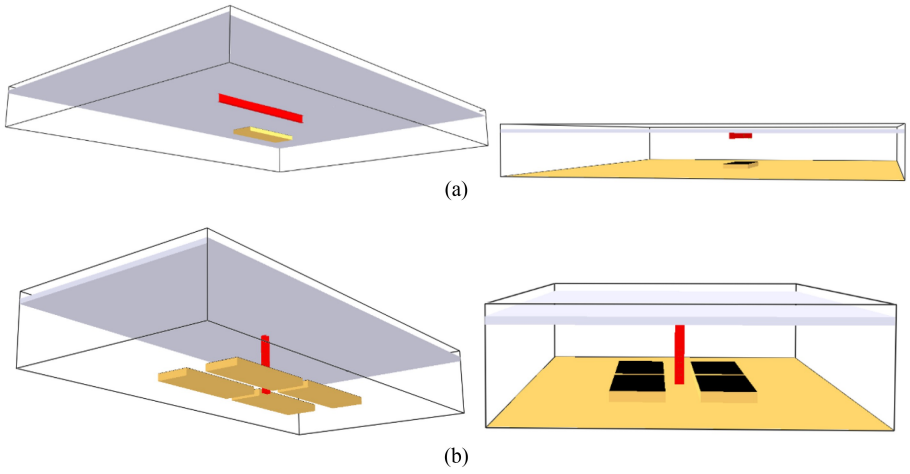

Fig. 6 FDS modeling domains for the open car park fire analyses. (a) Steel beam; (b) steel column.

point of the structural member.

The steel member temperatures are also investigated with the simple models described above. The burning car is modeled by a 3.2 m-diameter circular plan area with equivalent fire area. The axis of the localized fire is at the center of car. The heat release rate of the burning car is consistent with the heat flux curves in Figs. 3 and 4. In SAFIR, a flux constraint 'Hasemi' is available for the heat transfer analysis. It computes the flux applied to each point of integration (POI) of the steel beams based on the simple Hasemi model. This flux constraint is also applied to the upper part of the column, which is located inside the smoke layer. For the lower part of the column, the LOCAFI model is applied. SAFIR evaluates the flux using the solid flame model and assuming that the burning car is represented by a cone shape fire. For members in the axis of the flame, the Heskestad model is applied. The equations from Eurocode EN1991-1-2 are used to evaluate the flame temperature along the vertical axis of the fire. The heat flux to the member is then evaluated considering both the convective and radiative heat flux. It is worth noting that the Hesketad model is embedded in the flux constraint named 'LOCAFI' in SAFIR. With the flux constraint 'LOCAFI' applied, the heat transfer computation in SAFIR automatically shifts between the virtual solid flame model and the Heskestad model considering the relative position of the point of integration and the fire flame. When the point of integration is located in the flame, a convective flux with the flame temperature, and a radiative heat flux with this temperature, and a view factor of 1 are considered. The flame temperature is calculated by the Heskestad model in the centerline of the flame at the height of the POI. When the POI is located outside the flame, only the radiative heat flux is considered with the LOCAFI model.

3.3 Thermal analysis

Thermal analysis of the steel beam and column under open car park fires is conducted by finite element analysis using the software SAFIR [37]. A series of 2D thermal analysis of the cross section are carried out using solid conductive elements and capturing the convection and radiation at the boundaries. The equations to capture radiative and convective heat flux to the steel member are in accordance with Section 3 of the Eurocode EN1991-1-2 [32] and are detailed in Ref. [37]. Longitudinal variations in temperature distributions are captured by analyzing several cross-sections along the beam length; heat transfer in the longitudinal direction of the steel beam and column is neglected as the longitudinal dimension of the member is order of magnitudes larger than the thickness of the plates.

Different types of boundary conditions can be assigned to the steel sections in the thermal analysis. For the FDS-FEM AST method, the AST temperatures are applied to the surface of the cross section as temperature-time Frontier constraints. This boundary condition is the same as used when applying a temperature-time curve, e.g., from a standard fire curve or an OZone post-flashover model; except that here the temperature is the AST. For the FDS-FEM interface method, the transfer file is interpreted by SAFIR to compute heat flux at the boundaries (applied as Flux constraints in the thermal analysis). The treatment of the transfer file involves spatial and temporal interpolation as well as integration of the radiant intensities, which is completed by the software. For simple models, the thermal boundary condition is also applied as Flux constraints. Flux constraints are named either 'Hasemi' or 'LOCAFI' as detailed in Subsection 3.2 (with 'LOCAFI' encompassing both the virtual solid flame model and Heskestad model). For the simple models, a '.txt' file describing the fires has to be present in the calculation folder with an equivalent fire diameter of 3.32 m for each burning car. An input file describing the location of steel beam or column within the computational domain is also needed for the software to calculate the heat flux.

The thermal properties of the steel are in accordance with Eurocode EN1993-1-2 [27]. The conductivity and specific heat vary with the temperature. The convection coefficient is taken as 35 $W \cdot m^{-2} \cdot K^{-1}$, in accordance with Eurocode EN1991-1-2 for natural fire exposures [32]. Emissivity of the ungalvanized profiles is taken as 0.7. For the galvanized profiles, a newly developed material named GALVASTEEL is implemented in SAFIR. The new material GALVASTEEL emissivity is taken as 0.35 up to 500 °C and then 0.7 beyond 500 °C. A mesh size of 0.01 m is adopted for all the thermal analyses, as shown in Fig. 7. The thermal equilibrium equation is integrated in time to yield the evolution of the temperature distribution over the course of the fire. Time integration is conducted by the implicit single step scheme of the generalized central point, using a temporal integration parameter of 0.9 (1.0 represents a fully implicit scheme, while 0 represents explicit). The time step is set up as 5 s which allows the software to converge easily while the computational cost is reasonable.

4 Results

4.1 Temperature development in the beams

4.1.1 Fire scenario 1

The steel beam temperatures at the mid-span cross section under localized fire scenario 1 are shown in Fig. 8. Solid lines are used for the ungalvanized profiles, while dashed lines are used for galvanized profiles. The FDS-FEM AST method has been validated against test data in a previous study [15] and is thus used as benchmark.

For the car park fire scenario 1, both FDS-FEM methods yield similar results for the IPE450 profile, while the interface method is slightly more conservative than the AST method for the HE600A profile. This verifies that for the structures located at the ceiling level and right above the heat source, the interface method is applicable, as shown in Fig. 5 (B3). In the FDS interface simulation, the beam is not modeled in FDS, but the flat slab ceiling is. When comparing the member temperatures reached in different profiles, the IPE450 experiences temperatures higher by almost 120 °C than HE600A due to the higher section factor.

Both the AST method and interface method correctly yield reduced temperatures when the profile is galvanized. Due to galvanization, the peak temperature is reduced by 53 °C in the web, and 69 °C in the flange of IPE450 at the center section. As for the HE600A profile, the peak temperature is reduced by 68 °C in the web, and 73 °C in the flange at the center section. The time to reach the peak temperature is also delayed by about 1 min for IPE450 and 2 min for HE600A due to galvanization. This is consistent with the fact that a lower emissivity leads to reduced heat transfer at the boundaries of the steel beam.

Simple models are also adopted to predict the member temperatures. The center section of the beam is in the axis of the fire and at the ceiling level. For such situation, two analyses are completed. One simple model approach is to apply the Hasemi model. Strictly speaking, the Hasemi model only applies when the flame touches the ceiling, while in the early stage of the fire this is not the case. Evaluating the heat flux throughout the localized fire event with the Hasemi model ("Hasemi" flux boundary condition in SAFIR) is thus expected to yield conservative results. Another approach is to evaluate the flux based on the flame temperature from the Hesketad model. This second approach ("LOCAFI" flux boundary condition in SAFIR) evaluates the flame temperature along the vertical axis of the fire, then applies either the virtual solid flame model to compute radiative flux to the beam at the early stage of the fire when it is outside the flame, or computes the convective and radiative flux to

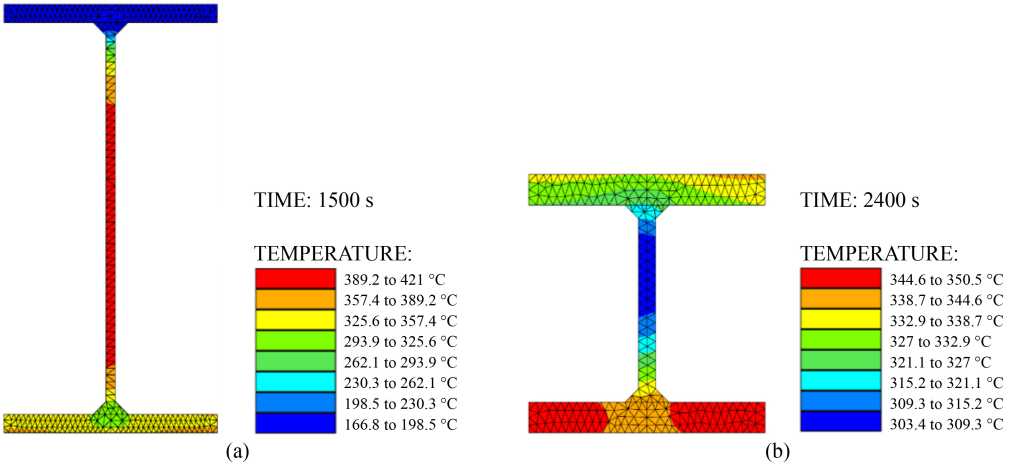

Fig. 7 Finite element thermal analysis. (a) Steel beam HE600A; (b) steel column HE240M.

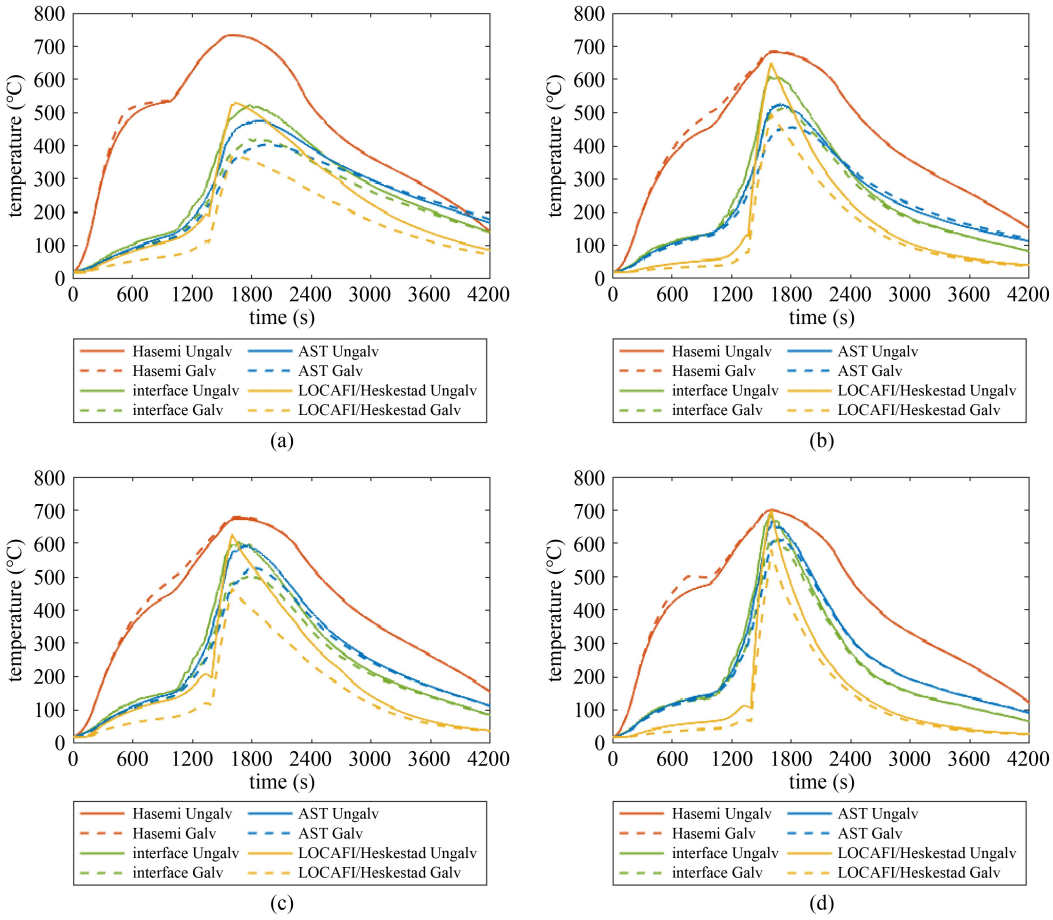

Fig. 8 Temperature evolution in the web and lower flange in fire scenario 1. (a) Lower flange of HE600A; (b) web of HE600A; (c) lower flange of IPE450; (d) web of IPE450.

the beam once it is inside the flame. In this second approach, the finite element software automatically transitions from the former flux computation to the latter based on the flame height. To indicate that both LOCAFI and Heskestad models are combined in this second approach, the curves in Fig. 8 are labelled as LOCAFI/Heskestad.

The Hasemi model significantly overestimates the steel temperatures, compared to the FDS-FEM AST/interface method. The overestimation is greatest during the initial heating phase. For example, at the 15th minute, the temperature difference between the Hasemi model and AST method reaches 420 °C in the lower flange of the ungalvanized HE600A profile, as shown in Fig. 8(a). A clear discrepancy in peak temperature between the Hasemi model and FDS-FEM models is also observed. For instance, the peak temperature difference between Hasemi model and AST method can be as much as 260 °C in the lower flange of ungalvanized HE600A profile, as shown in Fig. 8(a).

Another issue with the Hasemi model is that it erroneously represents the influence of galvanization on the member temperature. Contrary to the observation with FDS-FEM, Hasemi yields slightly higher steel temperature in the galvanized profile compared with the ungalvanized one. The causes for these shortcomings of the Hasemi model will be discussed in Section 5.

Regarding the LOCAFI/Heskestad model ("LOCAFI" flux boundary condition in SAFIR), during the initial stage when the HRR from the burning car is small and the analyzed section is outside the flame, lower temperatures are obtained compared with the FDS-FEM AST method. In this initial stage, the flux is computed based on the virtual solid flame, hence convection is neglected. After the flame touches the ceiling and the section is inside the flame, both the convective and radiative heat flux are taken into account, and evaluated based on the flame temperature from the Heskestad model. The model yields similar estimations of the peak temperatures reached in the profiles as the FDS-FEM AST method. The ability of the simple model to transition from virtual solid flame, when the steel member is outside the flame, to convection and the radiation phases when engulfed in flame, is clearly visible in the results. The sudden increase in temperatures that matches that obtained with FDS. It also captures the influence of galvanization with lower emissivity leading to lower temperature.

4.1.2 Fire scenarios 2 and 3

The steel beam temperatures at the mid-span cross section obtained from various methods under localized fire scenarios 2 and 3 are shown in Figs. 9 and 10. The FDS-FEM interface method yields lower member temperatures than the FDS-FEM AST method, especially at the lower flange. It is worth nothing that the steel beam is not modeled in FDS with the interface method, which means the impact of the presence of structural member on the fire development is neglected. The discrepancy in terms of the member temperature obtained with the FDS-FEM AST and interface method indicates that when the section is not right above the heat source (the burning car in scenario 2 or the second and third burning cars in scenario 3), the influence of the presence of the structural member cannot be neglected. Thus, the interface method is not recommended for this situation. Due to galvanization, the peak temperature is reduced by more than 60 °C for HE600A and IPE450 profiles in fire scenario 2. In fire scenario 3, the galvanization has less dominant effect on the peak temperature due to the more intense heating. The peak temperatures reached in fire scenario 2 are lower than those reached in fire scenario 1 due to the offset of the beam, while the peak temperatures reached in fire scenario 3 are higher than those reached in fire scenario 1 due to the higher heat release rate when three cars are burning instead of one. When comparing the member temperatures in different profiles, IPE450 experiences temperatures about 60 to 100 °C higher than the HE600A due to the different section factor.

The Hasemi model again overestimates the member temperatures compared with the FDS-FEM AST method. It is on the conservative side, with discrepancies not as large as for scenario 1, but still possibly making it overconservative for design. As observed previously, the Hasemi model also yields erroneous results on the effect of galvanization, because it cannot correctly capture the effect of a change in emissivity on the absorbed heat flux.

4.1.3 Comparison with experimental data

The CTICM conducted experiments on an open car park fire scenario similar to the scenario 3 in this study in 2000 [28]. Three Class 3 cars parked on three adjacent parking bays were involved in the test. The car in the middle was ignited first (for detailed information about the test, the reader is refered to Fig. 4.26 and Subsection 4.4 in the

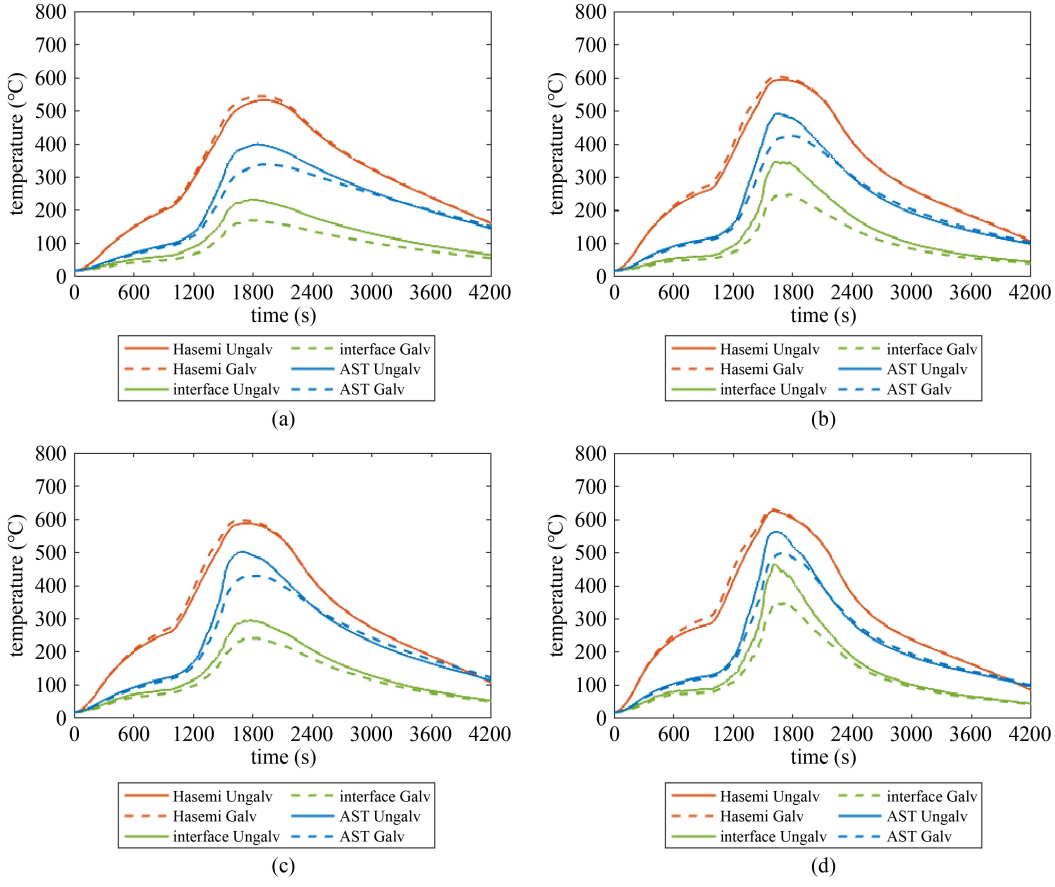

Fig. 9 Temperature evolution in the web and lower flange in fire scenario 2. (a) Lower flange of HE600A; (b) web of HE600A; (c) lower flange of IPE450; (d) web of IPE450.

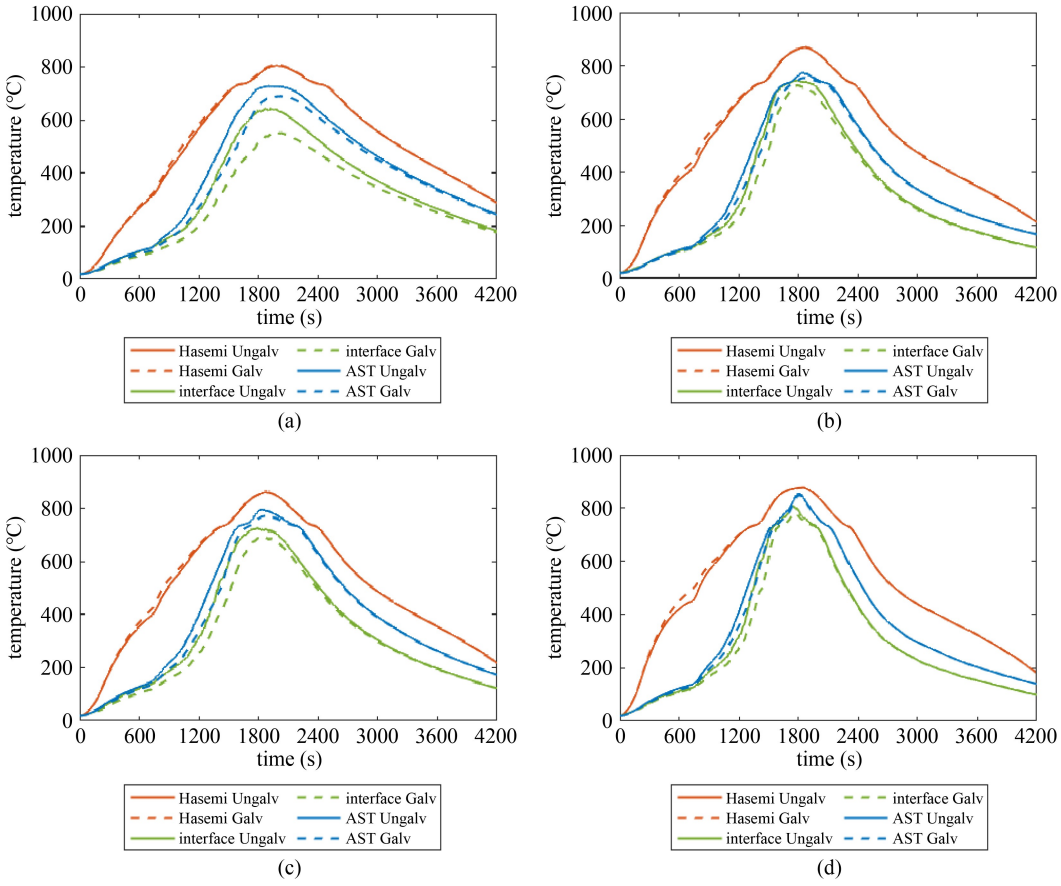

Fig. 10 Temperature evolution in the web and lower flange in fire scenario 3. (a) Lower flange of HE600A; (b) web of HE600A; (c) lower flange of IPE450; (d) web of IPE450.

test report [28]). The difference between the test and fire scenario 3 in this study is that the beam in the test was in the middle of two parking bays; it was thus not directly above a burning car but there was an offset. The maximum temperature in the tested IPE550 beam located between the first and second ignited car was around 700 °C at the mid-distance of a car. This value is comparable with the maximum temperatures of 772 and 855 °C computed with the FDS-AST methods in the webs of the ungalvanized HE600A and IPE450, respectively. The lower value obtained in the CTICM experiment compared to the numerical simulations in this study could be due to the offset of the beam in the test, while the simulation assumes a burning car directly underneath the axis of the beam.

4.2 Temperature development in the columns

The steel column temperatures in the flanges and web at 0.7, 1.9, and 2.4 m elevations under localized fire scenario 4, are shown in Fig. 11. The temperatures predicted by the FDS-FEM AST method are denoted by the solid lines, those predicted by the interface method are marked by the dotted lines, and those predicted by simple methods are presented by the dashed lines.

The heating sequence in the flanges is consistent with the fire propagation from the first car to the surrounding cars. The peak flange temperatures reached in points 1 and 4 are slightly higher than those in points 2 and 3. In terms of the modeling approaches, the FDS-FEM interface method yields slightly higher temperature in the flanges and web at different elevations of the column than the AST method. This discrepancy comes from the modeling strategy associated with the interface method that the steel column is not included in FDS simulation (while the steel column is included in the FDS simulation used with the AST method). It was shown in a previous study [15] that, when both the interface method and the AST method are applied to a case where the structural member is not included in FDS, they yield the same result.

For the lower part of the column (outside the smoke layer), the LOCAFI model yields lower member temperatures than the AST and interface methods, especially in the web, as shown in Fig. 11. For example, the difference of peak temperature from the AST method and the LOCAFI model can be as much as 200 °C in the web of the column at 1.9 m elevation. These results are discussed further in Subsection 5.3.

For the upper part of the column (inside the smoke

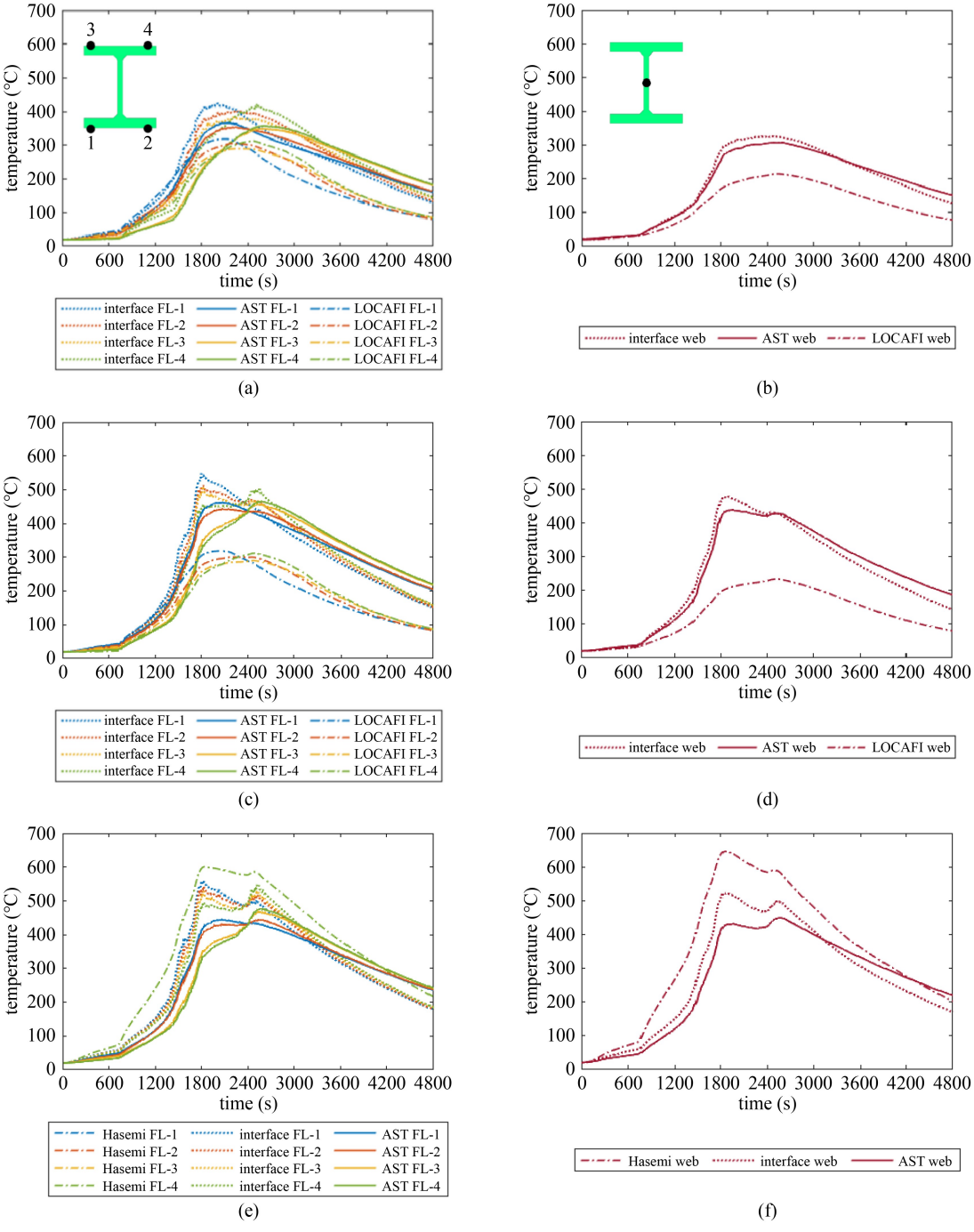

Fig. 11 Temperature in the HE240M in fire scenario 4. (a) Flange at the height of 0.7 m; (b) web at the height of 0.7 m; (c) flange at the height of 1.9 m; (d) web at the height of 1.9 m; (e) flange at the height of 2.4 m; (f) web at the height of 2.4 m.

layer), the Hasemi model yields higher member temperatures than the AST or interface method. The difference of peak temperature from the AST method and the Hasemi model can be as much as 175 °C in the flange of the column at 2.4 m elevation. Meanwhile, the Hasemi model is not able to capture the shadow effect and the whole section receives the same heat flux, thus the four flanges exhibit the same temperature, as shown in Fig. 11(e).

5 Discussion

5.1 Temperatures reached in the steel members

The peak and average temperatures obtained from the FDS-FEM AST method are summarized in Table 1. The peak temperature is taken as the maximum temperature reached on any cross section in the longitudinal direction of the structural members. The average temperature of the

Table 1 Peak and average temperatures of galvanized and ungalvanized profiles under localized fire scenarios (obtained from FDS-FEM AST method).

fire scenario	profile		peak temperature (°C)		average temperatures (°C)
	dimension	galvanization	flange	web	
1 (beam)	HE600A	Ungalva	476	526	428
		Galva	403	458	369
		difference	73	68	59
	IPE450	Ungalva	595	665	551
		Galva	526	612	494
		difference	69	53	57
2 (beam)	HE600A	Ungalva	400	491	355
		Galva	339	426	309
		difference	61	65	46
	IPE450	Ungalva	502	564	453
		Galva	430	500	397
		difference	72	64	56
3 (beam)	HE600A	Ungalva	728	772	671
		Galva	690	754	628
		difference	38	18	43
	IPE450	Ungalva	795	855	749
		Galva	770	848	718
		difference	25	7	31
4 (column)	HE240M	Ungalva	474	464	470
	(at z = 2.3 m)	Galva	425	420	412
		difference	49	44	58

steel beam is taken as the arithmetical average of the temperatures at the bottom of lower flange, center of lower flange, mid web, and bottom of upper flange, while the average temperature of the steel column is taken as the arithmetical average of the temperatures at the four flanges and the mid web, as shown in Fig. 12.

The size of the structural member and the location and number of burning cars influence the temperatures reached in the steel beam profiles. Under the same localized fire scenario, the peak temperature reached in the profile depends on the dimension of the profile, with higher peak temperature reached in more slender profile. In the fire scenario 1, the member temperatures in IPE 450 profile are generally 120 °C higher than HE600A, while in fire scenarios 2 and 3, the difference is more than 70 °C. The steel beam right above the burning car (scenario 1) experiences higher peak temperature than the one with an offset to the burning car (scenario 2). This difference can be as much as 60 °C for HE600A and 90 °C for IPE450. The peak temperatures reached in the profiles above three burning cars (scenario 3) are higher than those reached above a single burning car (scenario 1) due to the higher heat release rate with multiple burning cars. For example, the peak temperature at the lower flange of ungalvanized HE600A is increased from 476 °C under fire scenario 1 to 728 °C under fire scenario 3.

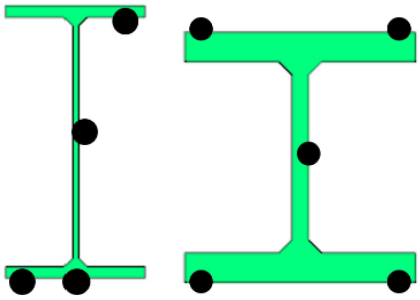

Fig. 12 Temperatures distribution on the cross section. (a) Steel beam; (b) steel column.

When subject to open car park fires, galvanization has the effect of delayed heating and reduced peak temperature. As listed in Table 1, the peak temperatures in HE600A are reduced by more than 60 °C and those in IPE450 are reduced by more than 50 °C under localized fire scenarios 1 and 2 when galvanization is applied to the steel members. The influence of galvanization on reduced peak temperature is less dominant in localized fire scenarios 3, see Fig. 13. This is because the zinc coating

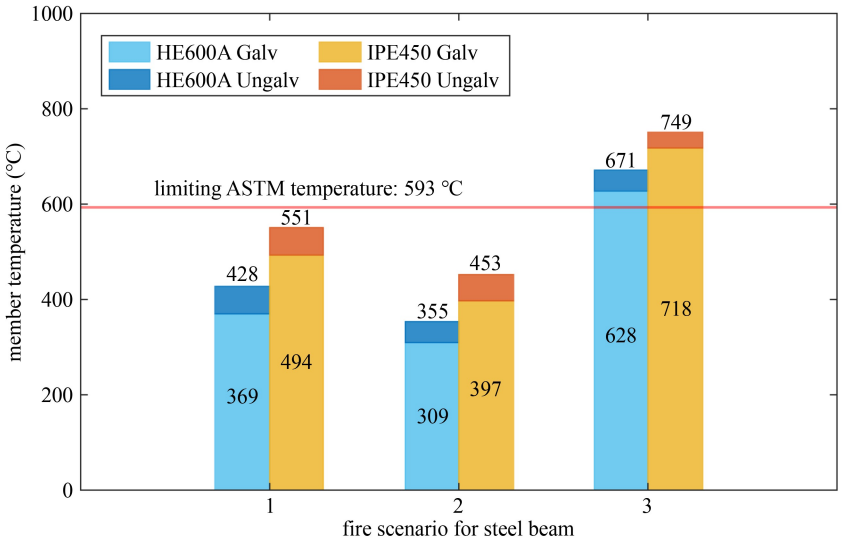

Fig. 13 Average temperatures reached in the critical section of the HE600A and IPE450 beams subjected to the open car park fire scenarios.

applied on the surface of the steel melts at a temperature of 500 °C, so the member temperatures gradually catch up with the fire temperature for severe fire exposures. For the steel column investigated in this study, the peak temperatures are reduced by more than 40 °C under localized fire scenario 4.

5.2 Limitations of the Hasemi model

Comparison of the temperature evolution in the steel beam at the ceiling level show that Hasemi model is more conservative than the FDS-FEM coupling methods. The main reasons of this noticeable difference are the following. 1) The Hasemi model assumes that the flame touches the ceiling. It is an empirical model where the flux is calibrated on an experiment during which the flame was touching the ceiling. Figure 14 shows the HRR cloud map captured at different time steps in the FDS simulation of localized fire scenario 1. It can be observed that the flame was not impacting the ceiling (grey block in Fig. 14) before 1000 s (growing phase in the HRR curve of class 3 car shown in Fig. 2) and after 1900 s (cooling phase) in the FDS simulation. In other words, as can be observed in FDS modeling, the flame touched the ceiling during only one sixth of the whole fire duration. 2) The Hasemi model was derived from experimental tests in which the ceiling was made of perlite boards. The energy absorbed by perlite boards was lower than that absorbed by the concrete slabs in a car park structure. The latter behave as a heat sink that absorbs a large amount of energy, which caused a decrease in gas temperature at the ceiling level. 3) The Hasemi model did not capture the shadow effect, i.e., all boundaries of the section received the same heat flux with the value calculated at the point of integration in FEM software. For open sections with concave parts, the received heat flux evaluated by the Hasemi model is therefore overestimated, which leads to higher member temperatures.

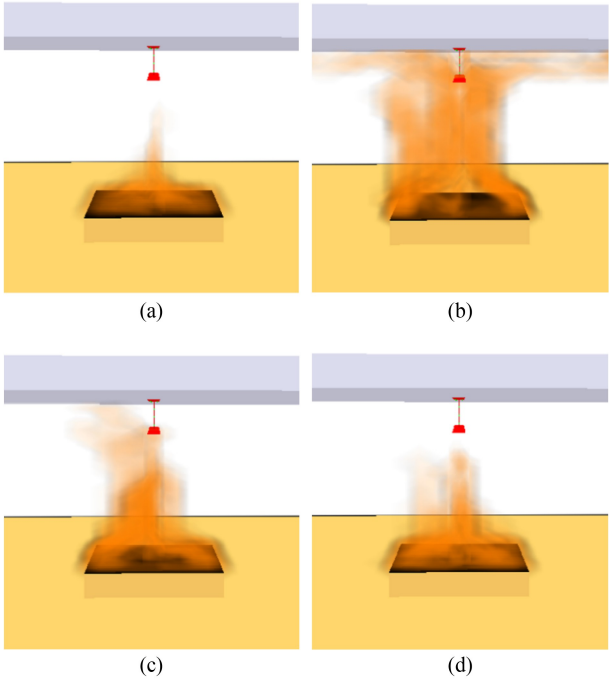

Fig. 14 HRR cloud map obtained from FDS simulation of the localized fire scenario 1 shows that the flame does not touch the ceiling (grey block) for most of the fire duration. (a) t = 1000 s (flame is not impacting ceiling); (b) t = 1500 s (flame is impacting ceiling); (c) t = 1700 s (flame is impacting ceiling); (d) t = 1900 s (flame is not impacting ceiling).

Besides, the Hasemi model gives erroneous results when applied to a material with different thermal properties than the ones for which the model was calibrated. More specifically, Hasemi model gives higher member temperatures with lower emissivity. This is due

to the fact that the heat flux given by the Hasemi model is in fact inherently an absorbed heat flux, meaning that it does not depend on the thermal properties of the receiving member (because it is already implicitly multiplied by the thermal properties of the material for which it was calibrated). When using the Hasemi model, the net heat flux on the boundary of a solid is evaluated with Eq. (1).

$$\dot{q}_{\text{net}} = \dot{q}_{\text{Hasemi}} - h_{\text{hot}}(T_{\text{s}} - T_{\text{amb}}) - \sigma\varepsilon(T_{\text{s}}^4 - T_{\text{amb}}^4), \quad (1)$$

where $\dot{q}_{\text{Hasemi}}$ is the flux computed according to Eq. (C.4) of EN 1991-1-2 [32] (incoming "absorbed" flux from the plume) [29]; h_{hot} is the coefficient of convection on exposed surfaces; T_{s} is the temperature at the surface of the solid at the boundary; T_{amb} is the ambient temperature; σ is the constant of Stefan Boltzmann; ε is the emissivity of the material of the solid. As can be seen in Eq. (1), the incoming (absorbed) part is independent of the thermal properties of the solid, whereas the outgoing (re-emitted) part depends on h_{hot} and ε.

In this study, the steel member is analyzed in two configurations: ungalvanized (ε = 0.7) and galvanized (ε = 0.35). The incoming flux $\dot{q}_{\text{Hasemi}}$ is the same for the two configurations, which does not capture the fact that reducing emissivity physically leads to less radiant heat absorbed in a solid. The outgoing flux, in contrast, accounts for the term ε and therefore will be larger for the material with larger emissivity (as the latter is able to re-radiate more heat to the far field as its temperature increases). The result is that the net heat flux on the boundary of the ungalvanized steel would be smaller than that of the galvanized steel. This contradicts the physics and erroneously leads to higher temperatures in galvanized steel members than in (otherwise identical) ungalvanized members.

5.3 Comparison between simple and advanced fire modeling approaches for columns

Figure 15 shows the effect of the four fire sources in scenario 4 in this study as simulated using FDS. Comparisons of the temperature evolution in the steel column surrounded by multiple localized fires show that the FDS-FEM coupling methods yield higher steel temperatures than the LOCAFI model, for the considered case study. The LOCAFI model was validated based on a series of experimental study, which included scenarios with steel columns surrounded by multiple pool fires [39], similar to the fire scenario 4 in this study. It was shown that the comparison between the LOCAFI model predictions and the average experimental values are largely safe-sided [8]. In the absence of measurements from full scale 4-cars column fire experiments, no conclusion can be drawn on the merits of the different approaches for steel column temperatures predictions, but this analysis allows to factually observe different temperatures obtained through the application of the different methods available.

For the upper part of the column near the ceiling level, the Hasemi model yields slightly more conservative prediction of the member temperatures than the FDS-FEM coupling methods.

5.4 Implications for performance-based fire design

The performance-based design approach has been increasingly adopted in recent years for the structural fire design of car parks. This approach provides several potential advantages over the traditional prescriptive design approach, including a more quantifiable level of safety and potential cost saving and design optimization [40,41]. It relies on rational analysis to explicitly evaluate the response of the structure in fire and then assess whether the design can achieve the required performance objectives. Thermal analysis, which evaluates the temperatures inside the structural member under certain fire exposure conditions, is a key step in the performance-based fire design procedure. The accuracy of the thermal analysis has a direct and significant impact on the following structural analysis. The structural analysis

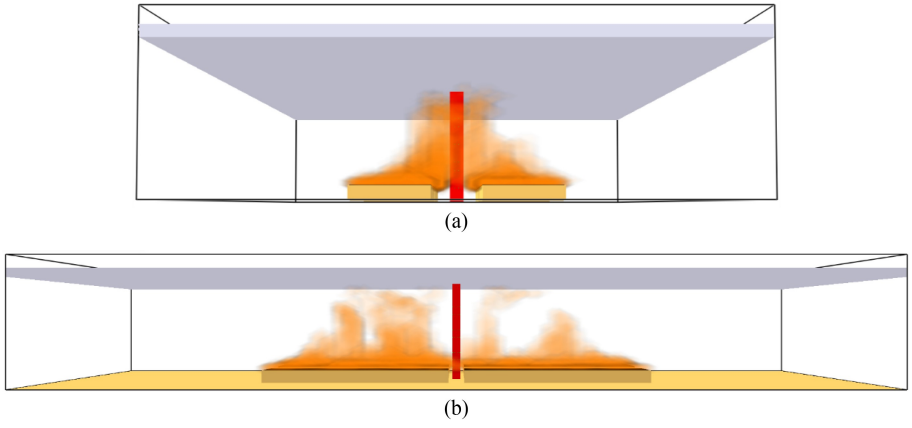

Fig. 15 FDS model of localized fire scenario 4 for steel column. (a) Front view; (b) side view.

adopts the temperatures from the thermal analysis in the assessment of the response throughout the fire exposure which eventually determines the required amount of fire protection for the steel members.

For reference, the temperatures obtained in this study can also be compared with the critical temperature specified in ASTM E119 standard [42] for a prescriptive design of structural members in fire. It is important to note that prescriptive and performance-based approaches should not be amalgamated for design. The prescriptive critical temperatures have limited relation to *in-situ* system performance, yet it is useful to compare the outcomes of the thermal analysis with these prescriptive temperatures as an indicative check. In the open car park fire scenarios 1 and 2, the peak temperatures in the investigated ungalvanized steel beams are lower than 704 °C and the average temperatures are lower than 593 °C, i.e., they would satisfy the prescriptive thermal requirements from ASTM E119 without thermal protection. However, when subjected to multiple localized fires (localized fire scenario 3), the temperatures are higher than the limiting temperature. As a result, the structural fire response of the structure needs to be assessed under these temperatures to check the structure performance. Completing a 3D FE model of the structure may demonstrate that the beams may be left unprotected through load redistribution in the structure (e.g., tensile membrane action of the composite floors [43]). In the localized open car park fire scenario 4, the average temperature of the steel column is lower than 538 °C and the peak temperature on any cross section is lower than 649 °C, suggesting that no thermal protection is needed for the steel column in a simple element approach. In general, completing a structural fire analysis is recommended to explicitly assess the response of the structure under fire exposure, as the limiting temperature criteria are a simplification intended for prescriptive design.

From the perspective of modeling approaches, both the simple models and advanced numerical modeling can be used for the performance-based fire design. Simple models tend to provide more conservative results and have limited field of applications, but they are generally computationally efficient. As an alternative to simple models, advanced numerical modeling approaches, especially the CFD-based models can provide more accurate results and can possibly enable optimization of the structure. For example, the peak temperature predicted by the Hasemi model in the upper part of the steel column under localized fire scenario 4 is 601 °C, while with the FDS-FEM AST method it is 474 °C. However, advanced numerical thermal analysis generally has higher demand on computational and modeling efforts.

6 Conclusions

This study focuses on the temperatures reached in steel framing members subjected to open car park fire scenarios. A parametric study was carried out considering the influence of the steel profiles, layout and number of burning cars, galvanization of the steel, and the modeling approaches adopted. The following conclusions are drawn.

1) The location and number of burning cars influence the peak temperature reached in the structural steel members. When subjected to a single car fire, the peak temperatures in the flange and web of the investigated beam profiles are higher when the beam is right above the burning car than when there is an offset. When subjected to multiple car fires, higher temperatures are reached in the steel beams compared to the case of a single burning car due to the higher heat release rate.

2) The temperatures in unprotected steel members under open car park fires may remain lower than the limiting temperature criteria specified in prescriptive fire design such as ASTM E119 throughout the entire fire event. This was the case for beams under single burning car fires and for the investigated column. This shows that localized fires generate thermal exposure conditions vastly different from those of standard (post-flashover) fires. As a result, it is often justified and allowed to adopt a performance-based structural fire design approach for open car park structures.

3) Structural fire design of open car park structures requires consideration of multiple car fire scenarios. The latter create thermal conditions more onerous than single car fires and generally lead to steel beam temperatures higher than the prescriptive limiting temperatures. Under these design scenarios, the computed temperatures can be used within a performance-based structural fire analysis based on three-dimensional FE modeling of the thermal-structural response. Since the thermal exposure from car fires is localized, it may be possible to leave the steel members unprotected through load redistributions in the structure, e.g., by designing to enable tensile membrane action in the composite floors.

4) When subject to localized open car park fire, galvanization has the effect of delayed heating and reduced peak temperature. The peak temperatures in the investigated steel beam profiles are reduced by more than 50 °C under one localized fire, but this effect is reduced when subjected to multiple localized fires because the steel temperature largely exceeds the melting temperature of the galvanization. In the investigated fire scenario for the steel column, the peak temperature is reduced by 44 to 49 °C.

5) In terms of modeling approach, the Hasemi model is overconservative in predicting the temperatures in the steel beams at the ceiling level under open car park fires.

This is mostly due to the assumption in the Hasemi model that flames are touching the ceiling during the whole fire duration, which contradicts observations from FDS modeling.

6) Another limitation of the Hasemi model is that, since it provides an absorbed heat flux, it incorrectly predicts that reduced steel emissivity leads to higher steel temperatures. Indeed, the predicted absorbed heat flux in Hasemi is independent of the emissivity but the reemitted heat flux decreases with a reduction in emissivity. In general, the Hasemi model cannot capture the effect of different thermal properties on the absorbed heat flux.

Future works could focus on further improvements of simple fire models for open car parks. Specifically, a unified simple model predicting the heat flux received by the different members of the structure would facilitate analyses. The estimation of the heat flux should capture the effect of the thermal properties of the receiving surface, unlike the current version of the Hasemi model. An important challenge is for simple models to capture the transition between different phases of the fire-structure interaction, including when the structural member becomes engulfed in the flame.

Acknowledgements This research was based in part upon work supported by ArcelorMittal Global R&D. This support is gratefully acknowledged.

Conflict of Interest The authors declare the following financial interests/personal relationships which may be considered as potential competing interests. Under a license agreement between Gesval S.A. and the Johns Hopkins University, Dr. Gernay and the Johns Hopkins University are entitled to royalty distributions related to the technology SAFIR described in the study discussed in this publication. This arrangement has been reviewed and approved by the Johns Hopkins University in accordance with its conflict of interest policies.

References

1. Zhao B, Roosefid M. Guide for Verification of the Fire Behavior of Largely Ventilated Car Parks with Metal Superstructure. CTICM document (SRI-11/110h-MR-BZ/NB), 2014 (in French)
2. Mangs J, Keski-Rahkonen O. Characterization of the fire behaviour of a burning passenger car. Part I: Car fire experiments. Fire Safety Journal, 1994, 23(1): 17−35
3. Macneil D D, Lougheed G, Lam C, Carbonneau G, Kroeker R, Edwards D, Tompkins J, Lalime G. Electric vehicle fire testing. In: 8th EVS-GTR Meeting. Washington, D.C.: National Research Council Canada, 2015
4. Zhao B, Kruppa J. Structural behaviour of an open car park under real fire scenarios. Fire and Materials, 2004, 28(24): 269−280
5. Joyeux D. Natural Fires in Closed Car Parks—Car Fire Tests. INC-96/294d-DJ/NB, 1997
6. Heskestad G. Engineering relations for fire plumes. Fire Safety Journal, 1984, 7(1): 25−32
7. Pchelintsev A, Hasemi Y, Wakarnatsu T, Yokobayashi Y. Experimental and numerical study on the behaviour of a steel beam under ceiling exposed to a localized fire. In: Fire Safety Science-Proceedings of the 5th International Symposium. Melbourne: IAFSS, 1997
8. Tondini N, Thauvoye C, Hanus F, Vassart O. Development of an analytical model to predict the radiative heat flux to a vertical element due to a localised fire. Fire Safety Journal, 2019, 105: 227−243
9. McGrattan K, Hostikka S, McDermott R, Floyd J, Weinschenk C, Overholt K. Fire Dynamics Simulator User'S Guide. Gaithersburg: NIST Special Publication, 2013
10. Alos-Moya J, Paya-Zaforteza I, Hospitaler A, Loma-Ossorio E. Valencia bridge fire tests: Validation of simplified and advanced numerical approaches to model bridge fire scenarios. Advances in Engineering Software, 2019, 128: 55−68
11. Alos-Moya J, Paya-Zaforteza I, Garlock M E M, Loma-Ossorio E, Schiffner D, Hospitaler A. Analysis of a bridge failure due to fire using computational fluid dynamics and finite element models. Engineering Structures, 2014, 68: 96−110
12. Guo Q, Root K J, Carlton A, Quiel S E, Naito C J. Framework for rapid prediction of fire-induced heat flux on concrete tunnel liners with curved ceilings. Fire Safety Journal, 2019, 109: 102866
13. Quiel S E, Yokoyama T, Bregman L S, Mueller K A, Marjanishvili S M. A streamlined framework for calculating the response of steel-supported bridges to open-air tanker truck fires. Fire Safety Journal, 2015, 73: 63−75
14. Hua N, Tessari A, Elhami-Khorasani N. Quantifying Uncertainties in the Temperature–Time Evolution of Railway Tunnel Fires. New York: Springer US, 2021
15. Yan X, Gernay T. Numerical modeling of localized fire exposures on structures using FDS-FEM and simple models. Engineering Structures, 2021, 246: 112997
16. Khan A A, Nan Z, Jiang L, Gupta V, Chen S, Khan M A, Hidalgo J, Usmani A. Model characterisation of localised burning impact from localised fire tests to travelling fire scenarios. Journal of Building Engineering, 2022, 54: 104601
17. Hidalgo J P, Goode T, Gupta V, Cowlard A, Abecassis-Empis C, Maclean J, Bartlett A I, Maluk C, Montalvá J M, Osorio A F, Torero J L. The Malveira fire test: Full-scale demonstration of fire modes in open-plan compartments. Fire Safety Journal, 2019, 108: 102827

18. Nadjai A, Naveed A, Charlier M, Vassart O, Welsh S, Glorieux A, Sjostrom J. Large scale fire test: The development of a travelling fire in open ventilation conditions and its influence on the surrounding steel structure. Fire Safety Journal, 2022, 130: 103575
19. Alam N, Nadjai A, Charlier M, Vassart O, Welch S, Sjöström J, Dai X. Large scale travelling fire tests with open ventilation conditions and their effect on the surrounding steel structure—The second fire test. Journal of Constructional Steel Research, 2022, 188: 107032
20. Fettah B. Fire Analysis of car park building structures. Thesis for the Master's Degree. Bragança: Polytechnic Institute of Bragança, 2016
21. Fang C, Izzuddin B A, Obiala R, Elghazouli A Y, Nethercot D A. Robustness of multi-storey car parks under vehicle fire. Journal of Constructional Steel Research, 2012, 75: 72−84
22. Sommavilla M, Tondini N. Fire performance of a steel open car park in the light of the recent development of the localised fire model "LOCAFI". In: The 11th International Conference on Structures in Fire. Brisbane: The University of Queensland, 2020
23. Zhang X G, Guo Y C, Chan C K, Lin W Y. Numerical simulations on fire spread and smoke movement in an underground car park. Building and Environment, 2007, 42(10): 3466−3475
24. Annerel E, Taerwe L, Merci B, Jansen D, Bamonte P, Felicetti R. Thermo-mechanical analysis of an underground car park structure exposed to fire. Fire Safety Journal, 2013, 57: 96−106
25. Tondini N, Morbioli A, Vassart O, Lechêne S, Franssen J M. An integrated modelling strategy between a CFD and an FE software: Methodology and application to compartment fires. Journal of Structural Fire Engineering, 2016, 7(3): 217−233
26. ECCS. Fire Safety in Open Car Parks: Modern Fire Engineering. European Convention for Constructional Steelwork, 1993
27. EN 1993-1-2. Eurocode 3: Design oF Steel Structures—Part 1-2: General Rules—Structural Fire Design. Brussels: European Committee for Standardization, 2005
28. Joyeux D, Kruppa J, Cajot L G, Schleich J B, van de Leur P, Twilt L. Demonstration of Real Fire Tests in Car Parks and High Buildings. EUR 20466. 2002
29. Cwiklinski C. Open Car Parks—Expert Opinion on Fire Scenarios Final report. INERIS DRA-CCw/MCh-2001-Cgr22984. 2001 (in French)
30. Collier P C R. Car parks—Fires involving Modern Cars and Stacking Systems. New Zealand, BRANZ Study Report 255. 2011
31. Cadorin J F, Franssen J M. A tool to design steel elements submitted to compartment fires—OZone V2. Part 1: pre-and post-flashover compartment fire model. Fire Safety Journal, 2003, 38(5): 395−427
32. EN 1991-1-2. Eurocode 1: Actions on Structures—Part 1-2: General Actions—Actions on Structures Exposed to Fire. Brussels: European Committee for Standardization, 2002
33. Wickström U, Duthinh D, McGrattan K. Adiabatic surface temperature for calculating heat transfer to fire exposed structures. In: Proceedings of the Eleventh International Interflam Conference. London: Interscience Communications, 2007
34. Wickström U, Hunt S, Lattimer B, Barnett J, Beyler C. Technical comment—Ten fundamental principles on defining and expressing thermal exposure as boundary conditions in fire safety engineering. Fire and Materials, 2018, 42(8): 985−988
35. CharlierM, Glorieux A, Dai X, Alam N, Welch S, Anderson J, Vassart O, Nadjai A. Travelling fire experiments in steel-framed structure: Numerical investigations with CFD and FEM. Journal of Structural Fire Engineering, 2021, 12(3): 309−327
36. Deckers X, Haga S, Tilley N, Merci B. Smoke control in case of fire in a large car park: CFD simulations of full-scale configurations. Fire Safety Journal, 2013, 57: 22−34
37. Franssen J M, Gernay T. Modeling structures in fire with SAFIR®: theoretical background and capabilities. Journal of Structural Fire Engineering, 2017, 8(3): 300−323
38. Gernay T, Kotsovinos P. Advanced analysis. In: International Handbook of Structural Fire Engineering. Cham: Springer, 2021, 413−467
39. Brasseur C, Zaharia M, Obiala R, Franssen R, Hanus J M, Zhao F, Pintea B, Sanghoon D, Vassart H, Nadjai O, Scifo A, Thauvoye A. Temperature Assessment of a Vertical Steel Member Subjected to Localised Fire (LOCAFI). EUR 28577. 2017
40. Yan X, Gernay T. Structural fire design of load-bearing cold-formed steel assemblies from a prototype metal building. Structures, 2022, 41: 1266−1277
41. Gernay T, Khorasani N E. Recommendations for performance-based fire design of composite steel buildings using computational analysis. Journal of Constructional Steel Research, 2020, 166: 105906
42. ASTM E119-18c. Standard Test Methods for Fire Tests of Building Construction and Materials. West Conshohocken, PA: ASTM, 2018
43. Vassart O, Bailey C G, Hawes M, Nadjai A, Simms W I, Zhao B, Gernay T, Franssen J M. Large-scale fire test of unprotected cellular beam acting in membrane action. Proceedings of the Institution of Civil Engineers, Structures and Buildings, 2012, 165(7): 327−334